Topiramate Induced Alteration in Frontal Lobe eLORETA-ICA Resting State Network Activity is Associated with Baseline Semantic Fluency Performance

A Thesis

SUBMITTED TO THE FACULTY OF THE

UNIVERSITY OF MINNESOTA

BY

Scott Luisi

IN PARTIAL FULFILLMENT OF THE REQUIREMENTS

FOR THE DEGREE OF

MASTER OF SCIENCE

Dr. Susan Marino

December 2020

Acknowledgements

Dr. Chris Barkley, for additional guidance, mentorship, and extensive work on editing and revising my manuscripts.

Dr. Pascal Faber and Dr. Nathanial Helwig for valuable correspondence regarding methodological questions.

This work was funded by NIH NINDS R01 NS076665; P.I. S.E Marino.

Abstract

Topiramate (TPM) is associated with a high rate of intolerable cognitive side effects that remain poorly understood and difficult to predict clinically. To investigate the underlying brain functions affected by TPM we applied eLORETA-ICA to resting state EEG data from 27 healthy subjects from both no-drug baseline and TPM study visits. Resting state independent component networks (ICs) were visualized and TPM related changes in network activity were identified with nonparametric paired permutation tests. Regression was then performed to associate baseline IC activity to changes in performance on neuropsychological test measures. We identified a subgroup of subjects defined by high baseline semantic fluency (SF) in whom: 1.TPM induced significant changes in prefrontal cortex activity in the high beta and gamma frequency ranges, and 2.baseline IC activity was associated with subsequent worsening in SF performance. This research shows eLORETA-ICA is a viable method of identifying drug-related changes in resting state network activity.

Table of Contents

List of Tables

List of Figures

Introduction

Topiramate (TPM) is a second-generation broad-spectrum anti-seizure drug (ASD) that, despite being efficacious[1–4] and commonly prescribed for focal and generalized seizures, also causes well-documented cognitive impairments in measures of attention, memory, and language in some patients.[5,6] Compared to other new ASDs, TPM has been shown to cause more frequent intolerable cognitive side effects, contributing to a higher rate of therapy discontinuation of an otherwise effective treatment.[7–9] Despite the widespread recognition of the prevalence of TPM-related cognitive impairment, a complete account of why some individuals experience these side-effects while others do not[8] remains elusive. Factors such as drug exposure, [5,10,11] baseline working memory capacity,[10,12] and spectral power in the Theta, Beta, and Gamma frequency bands of the resting state EEG[13] have been associated with the severity of cognitive deficits, but it is currently exceedingly difficult to reliably predict which patients will experience severe impairment.[10,12,14]

Part of the reason for this is that there is much we still do not understand about the neurophysiological mechanisms underlying TPM associated cognitive deficits. Ultimately, a greater understanding of the basic chemical and anatomical pathways that are impacted by TPM to cause adverse cognitive side-effects is necessary, but the type of basic science research required to obtain this information can be costly. A promising alternative way of investigating drug-related cognitive impairment in humans is by studying the effect of drugs on intrinsic/resting state brain networks (RSNs). The brain engages in spontaneous activity even when an individual is at rest with no external task/stimulus, (e.g. wakeful mind-wandering), and RSNs are sets of brain regions that exhibit correlations in this spontaneous activity.[15,16] Since the first RSN, the default mode network (DMN), was recognized in positron emission tomography (PET) and functional magnetic resonance imaging (fMRI) data, a number of different RSNs have been defined, such as the fronto-parietal network (FPN) and salience network (SN), and the relationship between activity in these networks both during task performance and at rest has been increasingly recognized as having important implications for cognition in healthy individuals and in disease states.[17–19] The DMN, for example, is a set of brain regions that show an increase in activity when an individual is at rest and a decrease in activity during externally focused tasks[19–21] and disruption of this expected pattern of DMN activity has been repeatedly associated with cognitive impairment and diseases where cognitive impairment is a hallmark symptom, including ADHD, schizophrenia, and Alzheimer's disease.[22–24] Furthermore, multiple investigations into the

effect of TPM on fMRI activation patterns have found evidence that TPM disrupts the expected patterns of task-related deactivation (TRD) of DMN brain regions during verbal fluency and working memory tasks, disruptions that have been theorized to contribute to impaired performance.[25–27]

In this study we used electroencephalography (EEG) data to investigate the effect of TPM on RSN activity; however, our understanding of the electrophysiology of RSNs remains relatively poor as attempts to establish a link between traditional EEG outcome measures such as spectral power and PET/fMRI-based RSN anatomical findings have historically produced inconsistent results.[28–32] Evidence from intracranial studies of resting state activity suggests one reason it has been challenging to study RSNs with scalp-level EEG may be that electrophysiological features of RSNs are too transient and/or spatially localized for traditional scalp-level EEG measures to reliably capture them.[33,34] As most studies of EEG-RSNs have relied upon relatively simple traditional EEG outcome measures, it may therefore be possible to identify reliable features of RSNs from surface EEG using analytical techniques that enhance the spatial resolution of the technique and/or identify patterns of coherent brain activity over time. In this study, to achieve these goals we relied on a combination of exact low-resolution electromagnetic tomography (eLORETA) and independent component analysis (ICA).

First, identifying the current source(s) inside the brain that create the scalp level signals seen in EEG recordings, termed the 'inverse problem', has long challenged mathematicians/neuroscientists.[35] Each electrode records a mixture of signals from a large number of local and distant current sources, so there are always multiple current source distributions that are mathematically consistent with the signals observed at the scalp.[35,36] eLORETA is an exact solution to the inverse problem with zero-error, at the expense of relatively low spatial resolution, producing an image of the standardized current density across the cortex based on electrical potentials measured from the scalp.[35,36] LORETA is one of many different approaches to calculating the inverse solution, and though other algorithms can achieve higher spatial resolution through more time consuming computation or by incorporating biophysiological constraints, when compared against these more computationally demanding solutions LORETA has been found to achieve results with spatial and temporal accuracy of <5 mm/5 ms respectively under most conditions.[35,36]

The second main technique in our analysis, which has played a large role in fMRI research into RSNs historically, is ICA.[37] Broadly, ICA is a hypothesis free mathematical decomposition method that reconstructs source activity by maximizing statistical independence.[38] This tool is a valuable way to identify patterns in complex datasets like those generated by fMRI or EEG. [39–41] For our purposes, a key quality of ICA is that when applied to subject groups and/or across experimental conditions as we have in this study it is able to extract patterns of activity that are represented across all groups/conditions.[39–41] Critically, this ensures that we are comparing the same patterns of brain activity before and after TPM administration in our statistical analysis.

A combination eLORETA-ICA approach has recently been used successfully by several groups to visualize and compare independent EEG-based RSNs.[42–44] Notably, Gerrits and colleagues were able to use this approach to reproduce the altered TRD of the DMN in patients with ADHD relative to healthy controls seen in prior fMRI studies and identify a component that was significantly correlated with inattention, a hallmark symptom of ADHD.[43] The eLORETA-ICA approach to investigating RSNs also allows us to extract information from the spectral domain, which has no equivalent in PET/fMRI data, to identify correlations in brain activity across any number of constituent frequency bands. Compared to the unidimensional nature of fMRI/PET data, EEG produces multidimensional data that is the summation of electrical oscillations across a number of constituent frequency bands that each have functionally/behaviorally relevant associations in the literature that we can draw upon when interpreting our results.[45–47]

In this study our primary objectives were to use the eLORETA-ICA approach to visualize and describe for the first time EEG based independent components (ICs) from combined pre-treatment baseline and TPM session resting state data, and to identify which ICs were sensitive to TPM by testing whether the relative amount of activity in each IC significantly changed after TPM administration. Finally, we aimed to identify whether activity in any TPM-sensitive ICs was associated with cognitive impairment on any sub-tests in our neuropsychological test battery.

Methods

Participants

Forty-six healthy right-handed volunteers gave written informed consent and completed all study visits. Exclusion criteria were: cardiovascular, endocrine, hematopoietic, hepatic,

neurologic, psychiatric, or renal disease; a history of drug or alcohol abuse within the past five years; the use of concomitant medications known to affect cognitive function (including antidepressants, anxiolytics, psycho-stimulants, analgesics, and antipsychotics); prior history of hypersensitivity to TPM, LZP, or related compounds; a positive pregnancy test (administered to all females before the start of each study visit); use of any investigational drug within the previous thirty days; a native language other than English; diagnosis of a speech and/or language impairment; uncorrected poor vision or hearing; and a dominant left hand (to control for brain lateralization of language). Nineteen subjects were excluded due to missing data resulting from technical issues with data acquisition or storage, leaving 27 for our analysis.

Study Protocol

The experimental protocol was approved by the Institutional Review Board of the University of Minnesota prior to the commencement of the study. We employed a double-blind, randomized, placebo-controlled crossover study design. Subjects signed informed consent, then completed a no-treatment baseline visit, during which they were familiarized with all study procedures and performed a modified Sternberg verbal working memory task[48]. Subjects were then assigned to one of six possible treatment sequences consisting of TPM, Lorazepam (LZP), and placebo (PBO) administered once each. At the next three visits, separated by two-week intervals, subjects' vital signs were checked before they randomly received either a single oral dose of TPM (subjects were randomized to receive either 100, 150, or 200 mg of TPM to induce a wide range of TPM concentrations across individuals), LZP (2 mg) or an inactive PBO, with drugs dispensed by the University of Minnesota Investigational Drug Services pharmacy.

Subjects completed a neuropsychological test battery at 0.5, 2.5, and 6 and between 24-96 hours after drug administration; we used data from the 2.5 hours post-dose time point in this study because it was closest to maximum TPM plasma concentration and directly preceding resting state EEG recording. Directly after the second neuropsychological test battery at 4 hours post dose resting state EEG was recorded prior to the working memory (WM) task paradigm. Blood draws were performed before dosing and at .5, 1.5, 2.5, 4, 6 and between 24-96 hours after dosing for quantification of TPM plasma concentration. Samples were immediately centrifuged, and the plasma frozen for future analysis. Drug plasma levels were quantified by liquid chromatograph-mass spectrometry (LCMS) assays.[49] The results of the primary study outcomes, including performance on the working memory test, comparison of the cognitive effects of

lorazepam and topiramate and pharmacometric analysis of the effects of TPM plasma concentration after controlling for other factors has been reported previously.[10,12]

The neuropsychological test battery included: the Controlled Oral Word Association (COWA) test[50] a test of phonemic verbal fluency that asks subjects to generate as many words as possible that begin with a specific letter over three 60-second trials; the descriptively named Semantic fluency (SF)[50] assessment is a test of categorical verbal fluency, which asks subjects to name as many items within a given concept/category (e.g. animals) as possible over a 60-second trial; the Trail making test (A & B)[51] tests cognitive control, task-set maintenance and alteration by having subjects trace a line between a series of numbered and/or lettered dots in ascending sequential order starting with 1/A; the Digit Span[52] (forward and backward) tests subjects' working memory maintenance and manipulation by asking them to memorize and repeat back (forward: original order, backward: reverse order) strings of digits that are read to them; and the Symbol digit modalities test (SDMT), which tests a subject's cognitive control and ability to sustain attention by requiring them to substitute or "decode" a series of randomized geometric shapes for their corresponding number based on a cypher, as quickly as possible. In the modified Sternberg WM task subjects were briefly presented a pronounceable nonsense syllable, followed by a 5s retention period, after which they were shown a probe syllable; subjects answered whether the probe syllable was the same as the cue syllable with a yes/no button press. A more detailed description and results from the WM paradigm have been reported in prior publications.[10,12]

EEG acquisition and preprocessing

We chose to limit our analysis to the final 3 minutes of the 4-minute eyes open (EO) passive fixation period prior to working memory task performance, excluding the first minute because it was found to be consistently noisy as subjects were still becoming settled and acclimating to the recording setup. The continuous data were first down sampled to 250 Hz and high pass filtered at 1 Hz. The data were cleaned in the following steps: bad channels were removed and subsequently re-interpolated, the data were re-referenced to the common average reference, 60 Hz line noise and its' harmonics were removed using the CleanLine plugin for EEGLAB[53], and the resulting data were entered into ICA. ICA was completed twice during preprocessing; artefactual components were rejected manually after both the first and second iterations of ICA.

Following preprocessing resting state EEG data were exported from EEGLAB for additional processing and LORETA analysis in the LoretaKEY software package (KEY Institute, University of Zurich, Switzerland). In an effort to balance computational limitations of our hardware with the data reduction effect of using epochs of greater duration the continuous resting state data were split into 30 second epochs, but due to subject movement/fatigue or technical issues with data acquisition in several cases less than 180 seconds could be obtained, so only 5 complete 30 second epochs were available from each subject and included in the ICA to maintain balance. Based on visual inspection of the electrode fit of our EGI Geodesic 129 electrode EEG cap (Electrical Geodesics, Inc. USA) to the default MNI152 head model[54], 21 non-cephalic electrodes (e.g. facial and electrodes proximal to the neck) were manually omitted, leaving data from 108 electrodes for our LORETA model.

eLORETA-ICA Analysis

After preprocessing, the cross-spectrum of each our 30s-epochs was calculated by applying a Fourier transform to the cross-covariance of the electrode level EEG signal. Significantly, it is in this step that each EEG epoch is transformed from the time domain to the frequency domain, becoming a measure of activity within each of 6 prespecified EEG frequency bands, which for this study were defined as: 1-3.5Hz delta; 4-7.5 Hz Theta; 8-13 Hz alpha; 14.5-20 Hz beta 1; 21-30 Hz beta 2; 31-47 Hz gamma.

The eLORETA algorithm was then run on the cross-spectra of each EEG epoch. The theory and derivation of the eLORETA algorithm used in this study have been described in great detail in prior publications.[36,55] Briefly, it is a linear weighted minimum inverse norm solution that models the cortex with 6239 voxels with 5 mm spatial resolution, and has been shown to have zero localization error under ideal no-noise conditions.[36,41,56]

Finally, we performed ICA on the cross-spectral images that were spatially localized using eLORETA, using voxel/frequency-wise scaling. We set the number of ICs to 12, based on the results of a sphericity test .[57] We included all subjects and both baseline and TPM study visits in our ICA to identify independent RSNs that exist (1) across all subjects and (2) in both study visits, but which may be more active in one condition than the other. To measure whether the level of activity in any of our identified ICs was significantly different between the baseline and TPM sessions the primary outcome variables were the epoch specific loading values for each IC output by the ICA algorithm. These values describe the degree to which brain activity

representative of that IC is present in a given epoch for a given study session. Z-transformed component images were visualized in the LORETA-KEY software with a Z-score threshold of >3.[42]

Statistics

All statistical tests were performed in R (version 4.0.2; R Foundation, Vienna, Austria). Nonparametric tests were performed using the nptest package[58], with additional custom coding implemented to perform block randomization as described by Winkler et al (2014, 2015).[59–61] The permutation method for location tests were sign flips, and both sign-flips and permutations for regression tests. The number of randomizations for both the location and regression tests were estimated using Monte Carlo standard errors when exact tests were not possible.

The group difference in IC activation between baseline and TPM sessions was tested using a nonparametric paired permutation test for the mean change in loading score (baseline loading – topiramate loading) from a null hypothesis of no change. A two-sided Johnson t-statistic was used to protect against the possibility of asymmetric error distribution. ICs with significant differences in mean activity between conditions (i.e. 'TPM sensitive') were carried forward in our analysis.

We first tested the association between activity in 'TPM-sensitive' ICs and cognitive impairment using multivariate nonparametric regression between loading scores and neuropsychological test scores. Heteroscedastic errors were conservatively assumed for all regression tests, so regression coefficients were tested for significance with the Wald test statistic. To reduce the number of neuropsychological tests included in the multivariate model the change in test scores between the placebo (PBO) and TPM were first tested with their own univariate paired permutation tests with Bonferroni correction for multiple comparisons; tests on which performance was significantly worse after TPM administration were considered for inclusion in the multivariate regression model. Note that for regression analyses the difference between TPM and PBO was used instead of the difference between TPM and baseline to control for session order and behavioral practice effects. Where there were multiple tests of the same neuropsychological domain (e.g. forward or backward digit span) only the most difficult variant was included in the regression (backwards digit span, Trails B).

We also performed post-hoc subgroups analyses; subjects were divided into high and low subgroups based on their baseline performance on the semantic fluency task. Creating subgroups based on semantic fluency task performance was decided upon because TPM is well-known to impair performance on this task, and prior literature suggesting TPM alters activity in cognitive brain networks during verbal fluency tasks.[25–27]A high baseline semantic fluency subgroup was defined as those subjects with greater than median semantic fluency scores at the baseline visit. We performed Bonferroni correction for the number of subgroup comparisons. Differences in subject demographics, TPM exposure, and session order between subgroups were tested with chi-square tests for categorical variables and one-factor ANOVAs for continuous variables.

Results

Identification of TPM-sensitive Independent Components

Tests to identify TPM-sensitive independent components were performed with 150,000 permutations, which corresponds to a Monte Carlo standard error [59] of .0001, with an accuracy of approximately 0.032 at a 95% confidence/.05 significance level. Paired tests of the difference of mean IC loading scores with the null hypothesis that $\mu_{bas,k\text{-}tpm,k} = 0$ for each of the K = 12 ICs generated by our eLORETA-ICA analysis revealed no results that were significant at the $\alpha = 0.05$ level.

Out of the 12 ICs generated by our eLORETA-ICA independent component #2 (IC2) and IC3 showed the largest mean differences between conditions, but compared to their respective permutation distributions, IC4 -923.3 (t = -2.92, p = 0.0917) and IC7 1083.8 (t = 3.38, p = 0.0977) were the only ICs found to be significant, albeit at the $\alpha = 0.1$ level, while IC2 -1620.4 (t = -3.06, p = 0.1118) was noted and retained for future analysis for possible trend-wise significance.

Determining the relationship between activity in TPM-sensitive IC(s) and TPM induced cognitive impairment

In addition to identifying ICs that were sensitive to TPM administration, we wished to investigate the relationship between IC activity and behavioral performance, beginning in the full cohort. Out of a number of neuropsychological tests we identified as potential candidates a priori, five tests whose scores significantly changed between the PBO and TPM conditions were chosen for inclusion in the initial regression model: change in PBO-TPM in overall working memory

accuracy, SDMT, backward DS, COWA, and SF. In the full cohort, using the Wald test statistic for the global null hypothesis that the change in ICA loading predicts the PBO-TPM change in all NP test score across all tests was profoundly insignificant for IC2 (W = 0.21, p = 0.99), IC4 (W = 2.2, p = 0.5), and IC7 (W = 1.18, p = 0.81). Based on prior literature[25–27] we performed regression including only individual measures of verbal fluency, but again no significant associations were observed for IC2, IC4 or IC7: SF (IC2 - W = 0.21, p = 0.67; IC4 – W = 2.25, p = 0.136; IC7 – W = 0.04, p = 0.86) or COWA (IC2 - W = 0.04, p = 0.86; IC4 – W = 1.6, p = 0.22; IC7 – W = 0.24, p = 0.65).

Identifying TPM-sensitive independent components in subjects with high baseline semantic fluency

We further investigated whether there may be subgroups of subjects for whom there was a significant change in IC activity due to TPM administration, focusing on IC2, IC4, and IC7. The high baseline SF group consisted of 13 subjects. Demographic characteristics of high and low SF subgroups can be seen in table 3. There were no significant differences in subgroup composition based on baseline demographics, TPM exposure, or session order (table 3).

The two subgroups showed markedly divergent effects across the retained ICs. In the high baseline SF subgroup the mean of the differences in loading scores between BAS and TPM sessions for IC2 was nearly 2x in magnitude (-3472.553, compared to -1620.352) than in the full cohort, corresponding to a p-value of 0.0095 in the same statistical test. Conversely, the high baseline SF subgrouping had the opposite effect for IC4 and IC7, for which the mean difference in loading scores between conditions was far less than the group as a whole. As expected, given the stark pattern displayed in the high baseline SF subgroup, the results in the low baseline SF subgroup were the opposite. IC2 had a much smaller mean difference of 99.55 (p = 0.95), while IC4 – -1575.08 (p = 0.092) and IC7 – 1734.35 (p = 0.12) showed larger differences.

To verify that this pattern in the SF subgroup was not a statistical anomaly, we attempted to demonstrate the specificity of IC2 to verbal fluency measures with two final tests in subgroups defined by high baseline values in a another verbal fluency measure, the COWA, as well as a neuropsychological test that is not considered related to fluency at all, the backwards DS. In the 13 subjects that made up the high baseline COWA subset the mean of the differences in loading was found to be -1798.17 (p = 0.078), which was not significant after correction for multiple comparisons (0.05 / 3 subgroups [SF, COWA, and backwards DS] = 0.01667). Finally, for

backwards DS, there were 15 subjects in the high baseline group (4 subjects shared the median score, so it was chosen to include them) and as expected the mean of the differences in loading for IC2 was not found to be significant: -634.72 ($p = 0.55$).

Determining the relationship between activity in TPM-sensitive IC(s) and TPM induced cognitive impairment in subjects with high baseline semantic fluency

We then performed our regression analysis again in the high baseline SF group. This regression model consisted of the baseline IC loading for IC2 as the predictor variable, and the PBO-TPM change in SF score as the response. Though the regression coefficient was small (β = 3.299517e-05) due to the difference of scale between IC loading and neuropsychological test score values, the association was found to be significant ($W = 5.7095$, $p = 0.0051$). When we attempted to add additional covariates to the model, starting with COWA scores (based on the expectation that COWA would be the neuropsychological measure most similar to SF), we found that while the overall p-value remained significant ($W = 5.71$, $p = 0.009$), the adjusted p-values for the individual regression coefficients showed that the addition of COWA to the model did not explain any additional variation (β_{COWA} = 4.424311e-06, $p=0.97$).

Discussion

In this double-blind cross-over study, we applied a combination eLORETA-ICA approach to resting state EEG data collected from subjects during both a no-drug baseline session and after administration of the ASD topiramate (TPM). Our research aimed to determine whether TPM significantly altered resting state network (RSN) activity in our cohort, and whether any observed changes were associated with impaired performance on any of our neuropsychological outcome measures. Our analysis showed that individuals with high semantic fluency (SF) at baseline experience a more dramatic change in the activity of the RSN(s) represented by our second independent component IC2, and that this change appears to be associated with how much their SF performance worsened when on TPM.

We identified 12 independent components (ICs) representing patterns of spectral-spatial activity that were consistent across both study visits for all subjects, theoretically constituting electrophysiological cross-frequency versions of the classical hemodynamic RSNs described in fMRI/PET literature.[15,16,41] Though these ICs represent activity from both no-drug baseline and TPM resting states, all ICs were not equally active in all subjects or study visits, and we were able to assess which networks displayed significant changes in activity in response to TPM

administration by contrasting group mean loading values between the no-drug baseline session and the TPM session.

In our primary analysis we identified three ICs with trendwise (p=0.1) or borderline trendwise significant change in loading values between study visits as being the most TPM-sensitive in our ICA: IC2, IC4, and IC7. It was when we tested the change in activity of our TPM-sensitive ICs again in in the high baseline SF subgroup that we observed a significant change in activity in IC2 between baseline and TPM sessions that was clearly absent in the corresponding low baseline SF subgroup. We further confirmed that in the high baseline SF subgroup there is a significant linear relationship between the TPM-related decrease in SF performance (the difference in SF score between PBO & TPM sessions) and baseline IC2 activity, whereas the low baseline SF subgroup shows no such relationship. We found no significant differences between the high and low baseline SF subgroups on any demographic or experimental factors we tested, supporting the generalizability of our findings and suggesting that TPM may have a differential effect on frontal brain networks (see figure 1) in individuals with a high level of SF than in those that perform lower on this measure.

Qualitative observations

Comparison to eLORETA-ICA literature

The eLORETA-ICA approach adopted here has recently been used to visualize and investigate the spatial and frequency distributions of brain activity in healthy subjects and ADHD patients,[42,43,62] and in our study it allowed us to visualize the effect of TPM administration on spatial-spectral RSNs in a manner previously only possible with fMRI.[37,39,63] However, the study of resting state networks across frequency bands with eLORETA-ICA is a relatively novel method, so there are few direct points of comparison for our results at the time of writing. Moreover, there are several potentially important differences in experimental design to take note of when comparing our work to the existing literature. Our study has been the first to attempt an eLORETA-ICA across no-drug baseline and drug conditions, and the impact of TPM on our ability to identify classical RSNs using eLORETA-ICA has not been established. Secondly, unlike our ICA, most other studies included active task conditions, such as the object-spatial-verbal cognitive style assessment in Milz et al[62], or the continuous performance attention task by Gerrits.[43]

Independent component 2

Among the ICs that showed trendwise significance in the full cohort (IC2, IC4, and IC7), IC2 (figure 1) is the only one in which we found a significant change in activity related to TPM in our high SF subset, but it also bears the least direct anatomical resemblance to any single RSN identified in the eLORETA-ICA literature.[42] Peak activity in IC2 in the middle frontal gyrus did not overlap with the frontal mPFC activation in the IC Aoki and colleagues attributed to the DMN in the same beta frequency band. Our IC2 extends much further across the superior frontal gyrus and is anticorrelated with a region centered on a portion of the medial frontal gyrus and extending across the ventromedial prefrontal cortex (vmPFC) and parts of the orbital gyrus and ventral ACC, which are also adjacent or overlapping with but do not appear to represent DMN nodes. The area of deactivation in the gamma frequency band of the IC Gerrits and colleagues found to be associated with attention task performance does show considerable overlap with the superior portion of IC2 in our data, but they also reported significant activation/deactivations in the delta, theta, and alpha bands.[43] Thus, there does not seem to be any direct analogue in the eLORETA-ICA literature to IC2, suggesting it may represent a combination of multiple networks or a novel eLORETA-ICA network not previously described in the literature.

Independent Component 4

Interpretation of IC4 (figure 2) also remains somewhat unclear, but this IC may correspond to a portion of the dorsal visual pathway (DVP), given the general pattern of occipital activity. The foci of deactivation however is centered around the postcentral gyrus, an area associated with auditory sensation/processing, as well as the primary motor cortex and the insula, and overlaps the lateral sulcus into transverse temporal areas that are part of the primary auditory cortex as well, making it unclear where this IC should be localized.[64] Based on this we can generally conclude that IC4 represents visual/auditory processing pathways that are either active/or suppressed in the resting state recording.

Independent Component 7

Meanwhile, our IC7 (figure 3) was composed of commonly seen occipitoparietal alpha frequencies[47] and almost directly aligns both in frequency and in spatial distribution to ICs described by Aoki[42] and Milz[62], and appears to be reflect activity in components of the ventral visual pathway (VVP) and/or the dorsal stream of language processing[65] with additional areas of

deactivation in the precuneus and spreading into somatosensory/motor and premotor areas at the top of the cortex. Interestingly, Milz and colleagues' analogue was similar but with a reversed pattern of activation/deactivation. This may be explained by the task-condition in their study, which they used to demonstrate that IC loadings in their analogue to IC7 were higher during object-visualization and verbalization compared to spatial visualization or resting.[62]

Spectral distribution of IC2 & IC4

IC2 and IC4 were composed predominantly of high frequency EEG oscillations in the high beta (21-30 Hz) and gamma (31-47 Hz) bands, which is consistent with observations of prior analyses of this cohort[13], and with previous work that attempted to identify a dominant EEG frequency band in different cortical areas during the resting state that reported beta in the middle frontal and inferior frontal gyri (IFG) (IC2), and the pericentral region (IC4).[47] However, in both IC2 and IC4 peak activity was actually found in the gamma frequency band, and we found no precedent in the eLORETA-ICA literature that adequately explains the prevalence of gamma in our ICs. However, gamma spiking has previously been observed in the primary visual cortex, and more generally transient oscillatory synchronization between gamma and other frequency bands is often thought of as playing a pivotal role in integration of sensory information, attention, and communication across brain networks.[33,45,46] Therefore, the high beta and gamma frequencies in IC2 and IC4 are not unexpected, and could indicate a role in cross-network synchronization/communication, but additional research into the cross-frequency coupling of RSNs is required to make any firm conclusions.

Comparison to fMRI resting state networks

In the larger body of fMRI RSN literature we find some precedent for the network we observed in IC2 in work by Smith and colleagues, who used an ICA model on a large database of resting fMRI data to generate resting state networks that they then compared to various associated cognitive domains identified in the source database.[63] Component (#8/20), which they described as an "executive control" network, includes both the superior and ventral components of our IC2, including the ACC, and was distinct from another IC they identified as the DMN.[63] In their analysis component #8 was associated with action inhibition, cognition/working memory, and emotion paradigms, as well as the perception of pain. Previous work in mice has also shown the dmPFC region to be involved in top-down inhibition of motor cortex during the delay period, but not the motor response, which aligns with the goals of our subjects in our resting state

recording.[66] Others have reported functional connectivity between the orbital gyrus and vmPFC and posterior brain regions involved in language, including the angular gyrus, parahippocampal gyrus and hippocampus proper, or the precuneus and posterior cingulate cortex (PCC), which form the central posterior hub of the DMN, offering a potential indirect route through which activity in IC2 could be associated with language performance downstream.[67,68]

Interpretation

We can conclude that the spectral distributions of IC2 and IC4 are broadly consistent with commonly observed frequency distributions or at least not without precedent in the literature, and that additional research to establish a base of knowledge regarding the spectral-spatial characteristics of RSNs is required. We hypothesize that IC4 and IC7 represent components of the occipitoparietal DVP and VVP/dorsal stream of language processing respectively, however localization of the anterior portion of IC4 remains unclear. Furthermore, we have no explanation as to why IC7 was not found to have a significant association to TPM in the high baseline SF subset over IC2 given the apparent association to brain areas known to be involved in language processing. While we observed no significant effects of TPM on activity in IC7 in the whole group or in subgroup analyses, the observation of corresponding networks in both Aoki and Milz does imbue confidence in the validity of our eLORETA-ICA approach overall. Based on the sum of outside literature, particularly fMRI classification of an executive control network that closely aligns with our IC2 we speculate that the effect we observed is associated with an alteration in networks involved in top-down executive control and response inhibition, that persisted outside of the resting period and negatively impacted subject's task performance.

Limitations

One of the primary limitations in our study was the sample size, which was at least 3x smaller than in the preceding eLORETA-ICA studies that our analysis was based on.[42–44,62] Our study suggests that it is possible to obtain valid and informative results with a much smaller sample size, but ultimately the ability of ICA to identify consistent patterns of activity across a group is proportional to the amount of data available to the algorithm. In addition, recording EEG in participants that were heavily sedated by the drug led to an increased number of artifacts in our data, necessitating rigorous cleaning during preprocessing. Both of these factors reduced the likelihood of the ICA identifying consistent RSNs across subjects and conditions.

In addition, EEG was only captured before the Sternberg working memory task, which occurred ~1.5 hours subsequent to the start of the neuropsychological test battery. We expect our group level analysis should have compensated for intraindividual variability (e.g. in difference in TPM levels, random variation in RSN activity in the interim)to some degree, however ideally the resting state recordings should have been more proximal to the neuropsychological tests that we used in this study.

Another limitation of our study design was our lack of MRI or other imaging of subjects' actual cranial anatomy. We relied upon the default MNI152 head model, which is a template and not representative of the individual subjects in our study. Ideally, individual patient anatomy would be taken into account to allow more precise estimation of current flow and localization of activity to the correct brain structures. Given natural interindividual neuroanatomical variability, the precise locations of our generated ICs must be interpreted with some caution.

We must also acknowledge the potential selection/retention bias present in our sample; we retained only those subjects with resting EEG available from both sessions, and noisy or messy data in subjects who experienced the most severe impairment during the TPM session in particular led to missing data in some subjects.

Future Directions

Additional studies that are prospectively designed to measure the effect of TPM on RSN's in a larger cohort must be performed to validate the significant subgroup effects we observed in this study, and to reexamine the borderline significant effects we observed on occipitoparietal networks represented in IC4 and IC7. Particularly, it will be important to confirm whether baseline SF performance is a reliable identifier of subjects in whom TPM will significantly alter activity in what we hypothesized was a frontal executive network (IC2). Future work should also aim to validate whether baseline activity in this network are consistently predictive of subsequent worsening in SF performance while on TPM.

One of the primary long-term goals of work such as ours is determining the potential utility of EEG based biomarkers for predicting drug efficacy and adverse response.[69,70] In clinical practice it remains challenging to predict which individuals are more likely to experience cognitive side effects after TPM administration, and in general there is a shortage of guidance on the matter for clinicians to make this decision. As a diagnostic method resting state EEG has

qualities of an ideal clinical biomarker, including being non-invasive, relatively cheap, and easy to perform in comparison to fMRI or PET, and resting EEG has been a well-established diagnostic tool used in epileptology for nearly a century.[71] The type of resting state EEG analyses we performed in this study are the first step towards establishing EEG-behavior relationships that could be translated into clinical decision making in the future.

Conclusion

After an initial failure to identify significant drug effects, our first post-hoc subgroup analysis identified a subgroup of subjects defined by high baseline SF in whom TPM induced significant changes in PFC activity in the high beta and gamma frequency ranges. We further found preliminary evidence suggesting baseline activity in these regions of the PFC may be associated with subsequent worsening of SF while on TPM. Based on our review of the literature the IC capturing this PFC activity may represent an "executive control" network involved in response inhibition as well as working memory; our results provide a convincing rationale for future studies into this RSN and its ability to identify individuals who are at risk of experiencing TPM induced cognitive impairment. From a methodological standpoint, our study provides a proof of concept, demonstrating that even in our relatively small sample size with severely noisy data the eLORETA-ICA approach produced ICs that were broadly in line with known patterns of brain activity/RSNs and allowed us to successfully identify drug-related changes in RSN activity.

Table1: Results from the nonparametric paired tests of the difference of mean IC loading scores

IC #	Mean of the Differences in IC loading	P-value (t-statistic)
4	-923.3185	0.0917 (-2.9186)
7	1083.789	0.0977 (3.3814)
2	-1620.352	0.1118 (-3.0603)
3	1531.133	0.1789 (2.8375)
8	996.3036	0.2499 (2.4061)
6	570.4837	0.278 (1.8329)
1	-583.2511	0.5173 (-1.8498)
9	453.3333	0.5527 (1.2487)
10	-452.1615	0.6358 (-0.8649)
5	-416.7929	0.6876 (-0.8116)
11	-115.0563	0.8362 (-0.3707)
12	-142.2519	0.8869 (-0.2441)

Table 2: Difference of Mean IC 2 Loading Scores in SF Subgroups

Full cohort (n=27)

IC	mean of the differences	p-value	t-stat
2	-1620.352	0.1118	-3.06
4	-923.3185	0.0917	-2.9186
7	1083.789	0.0977	-3.3814

High Baseline SF subgroup (n=13)

IC	mean of the differences	p-value	t-stat
2	-3472.553	0.0095	-5.9237
4	-221.4252	0.7512	-0.5186
7	383.187	0.6113	0.9926

Low Baseline SF subgroup (n=14)

IC	mean of the differences	p-value	t-stat
2	99.55	0.95	0.1199
4	-1575.077	0.0921	-3.5114
7	1734.349	0.1148	3.4494

Table 2: Comparison of full cohort versus high and low baseline SF score subgroups in nonparametric paired tests of the difference of mean IC 2 loading score.

Table 3: Baseline Characteristics of High and Low SF Subgroups

	Baseline SF subgroup	low subgroup	high subgroup	p-value
Gender				1
	Male	7	7	
	Female	7	6	
Dose				0.354
	100mg	3	6	
	150mg	5	4	
	200mg	6	3	
Race				0.4753
	Asian	1	1	
	Black	2	1	
	Multiracial	2	0	
	White	9	11	
Education				0.2101
	High school graduate	1	0	
	Completed vocational training	11	7	
	Some college	2	4	
	Any post-graduate education	0	2	
treatment order				0.1469
	1	2	3	
	2	3	1	
	3	0	4	
	4	4	1	
	5	2	3	
	6	3	1	
TPM Plasma concentration @ the 2.5-hour draw, Mean (SD)		2.89 (0.91)	2.15 (1.08)	0.0645
Weight, Mean (SD)		78.29 (14.70)	79.95 (14.38)	0.77
Age, Mean (SD)		25.98 (9.75)	25.63 (7.09)	0.915

Table 3: Baseline subgroup comparison of demographic and experimental factors – categorical variables are tested via Pearson Chi-Square test, continuous variables were tested via univariate ANOVA.

Figure 1: Independent Component #2

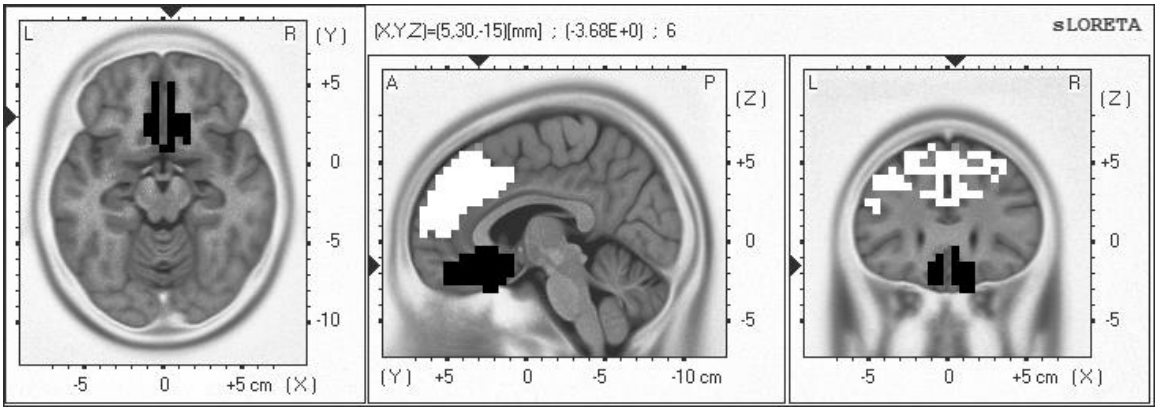

Figure 1: Z-transformed image of IC2 in the gamma frequency band with Z-score threshold of >3. White corresponds to positive current density vector field power and black corresponds to negative current density vector field power. IC2 consists of activity in bilateral and dorsolateral and dorsomedial prefrontal cortices (Brodmann areas 8-10) in beta2 and gamma frequency bands, which was anticorrelated with activity that peaked in the ventral medial prefrontal (vmPFC) (Brodmann 11, 25) and spanned the orbital gyrus, the medial frontal gyrus and anterior cingulate cortex.

Figure 2: Independent Component #4

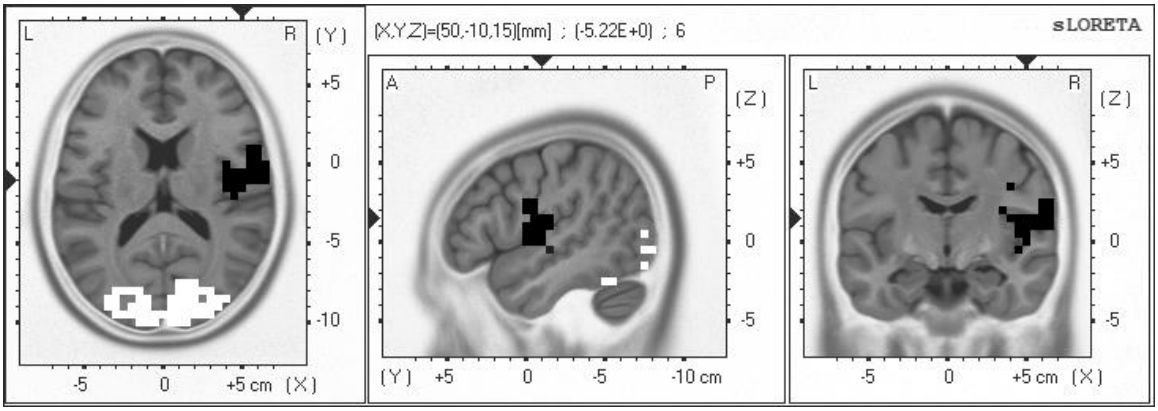

Figure 2: Z-transformed image of IC4 in the gamma frequency band with Z-score threshold of >3. White corresponds to positive current density vector field power and black corresponds to negative current density vector field power. IC4 appears as activity in primary visual and visual association areas of the occipital cortex (Brodmann areas 17 & 18) in beta2 and gamma which is anticorrelated with activity in the right precentral gyrus, superior/transverse temporal gyrus, and insula (Brodmann areas 4, 6, 13, 22, 41-44).

Figure 3: Independent Component #7

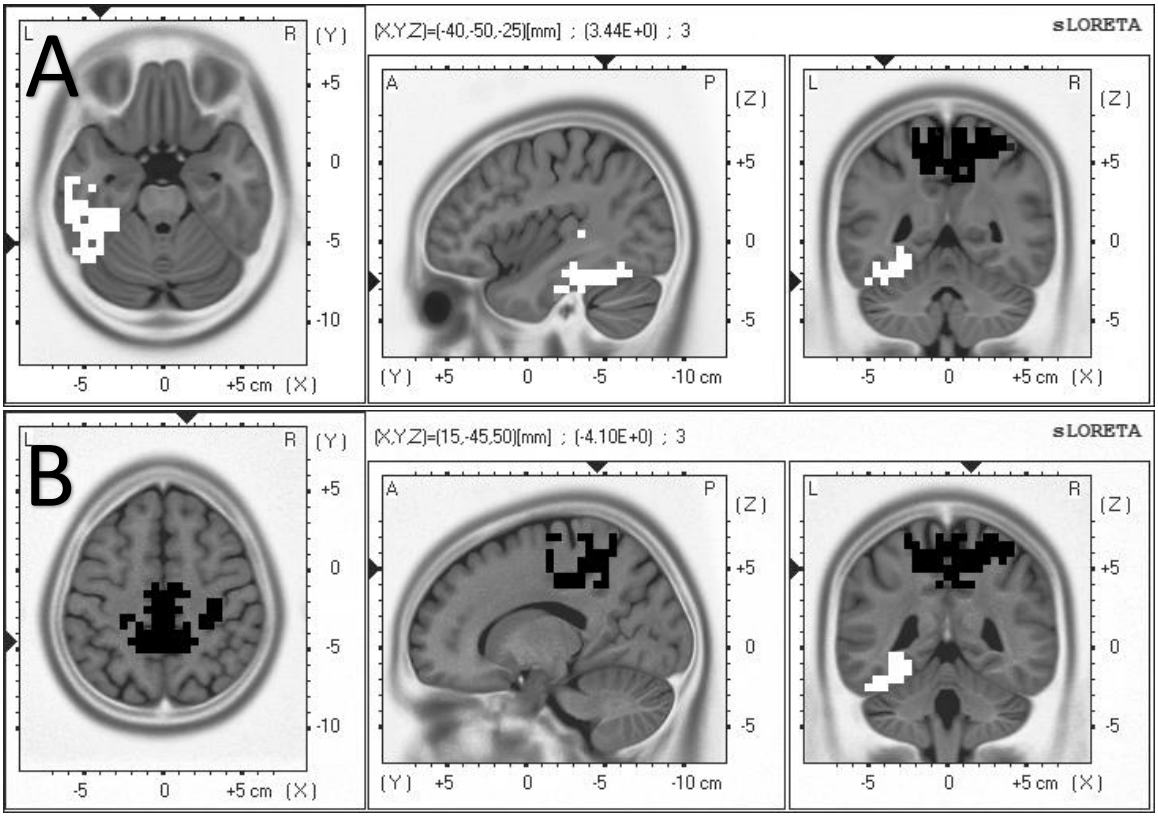

Figure 3: Z-transformed images of IC7 in the alpha frequency band with Z-score threshold of >3 at the maximum (A) and minimum (B) points. White corresponds to positive current density vector field power and black corresponds to negative current density vector field power. Significant activity in IC7 is found exclusively in the alpha frequency band, with the absolute extreme in the precuneus (Brodmann area 7), but this deactivation extends into the precentral (Brodmann area 4) paracentral (Brodmann areas 6, 31) and postcentral gyri (Brodmann area 3). This is anticorrelated with activations in the left inferior temporal/fusiform gyrus region (Brodmann area 20, 36, 37), the left parahippocampal gyrus (Brodmann area 19), and superior temporal gyrus (Brodmann area 22).

Bibliography

1. Brandes JL. Topiramate for Migraine PreventionA Randomized Controlled Trial. *JAMA*. 2004;291(8):965. doi:10.1001/jama.291.8.965

2. Faught E, Wilder BJ, Ramsay RE, et al. Topiramate placebo-controlled dose-ranging trial in refractory partial epilepsy using 200-, 400-, and 600-mg daily dosages. *Neurology*. 1996;46(6):1684-1690. doi:10.1212/WNL.46.6.1684

3. French JA, Kanner AM, Bautista J, et al. Efficacy and tolerability of the new antiepileptic drugs I: Treatment of new onset epilepsy: Report of the Therapeutics and Technology Assessment Subcommittee and Quality Standards Subcommittee of the American Academy of Neurology and the American Epilepsy Society. *Neurology*. 2004;62(8):1252-1260. doi:10.1212/01.WNL.0000123693.82339.FC

4. Silberstein SD. Topiramate in Migraine Prevention: Results of a Large Controlled Trial. *Archives of Neurology*. 2004;61(4):490. doi:10.1001/archneur.61.4.490

5. Marino SE, Pakhomov SVS, Han S, et al. The effect of topiramate plasma concentration on linguistic behavior, verbal recall and working memory. *Epilepsy & Behavior*. 2012;24(3):365-372. doi:10.1016/j.yebeh.2012.04.120

6. Mula M, Trimble MR, Thompson P, Sander JWAS. Topiramate and word-finding difficulties in patients with epilepsy. *Neurology*. 2003;60(7):1104-1107. doi:10.1212/01.WNL.0000056637.37509.C6

7. Arif H, Buchsbaum R, Weintraub D, Pierro J, Jr. SRR, Hirsch LJ. Patient-reported cognitive side effects of antiepileptic drugs: Predictors and comparison of all commonly used antiepileptic drugs. *Epilepsy & Behavior*. 2009;14(1):202-209. doi:10.1016/j.yebeh.2008.10.017

8. Bootsma HP, Ricker L, Hekster YA, et al. The impact of side effects on long-term retention in three new antiepileptic drugs. *Seizure*. 2009;18(5):327-331. doi:10.1016/j.seizure.2008.11.006

9. Chung S, Wang N, Hank N. Comparative retention rates and long-term tolerability of new antiepileptic drugs. *Seizure*. 2007;16(4):296-304. doi:10.1016/j.seizure.2007.01.004

10. Callisto SP, Illamola SM, Birnbaum AK, et al. Severity of Topiramate-Related Working Memory Impairment Is Modulated by Plasma Concentration and Working Memory Capacity. *The Journal of Clinical Pharmacology*. 2020;60(9):1166-1176. doi:10.1002/jcph.1611

11. Loring DW, Williamson DJ, Meador KJ, Wiegand F, Hulihan J. Topiramate dose effects on cognition: A randomized double-blind study. *Neurology*. 2011;76(2):131-137. doi:10.1212/WNL.0b013e318206ca02

12. Barkley CM, Hu Z, Fieberg AM, et al. Individual Differences in Working Memory Capacity Predict Topiramate-Related Cognitive Deficits: *Journal of Clinical Psychopharmacology*. 2018;38(5):481-488. doi:10.1097/JCP.0000000000000949

13. Barkley CM. Resting State Submission. *Epilepsy & Behavior*. Published online Accepted 2020.

14. Babu Henry Samuel I, Barkley C, Marino SE, et al. Brain's compensatory response to drug-induced cognitive impairment. *Journal of Clinical and Experimental Neuropsychology*. 2018;40(10):1000-1012. doi:10.1080/13803395.2018.1458822

15. Fox MD, Snyder AZ, Vincent JL, Corbetta M, Raichle ME. The human brain is intrinsically organized into dynamic, anticorrelated functional networks. Published online 2005:6. doi:10.1073/pnas.0504136102

16. Fox MD, Raichle ME. Spontaneous fluctuations in brain activity observed with functional magnetic resonance imaging. *Nature Reviews Neuroscience*. 2007;8(9):700-711. doi:10.1038/nrn2201

17. Anticevic A, Cole MW, Murray JD, Corlett PR, Wang X-J, Krystal JH. The role of default network deactivation in cognition and disease. *Trends in Cognitive Sciences*. 2012;16(12):584-592. doi:10.1016/j.tics.2012.10.008

18. Broyd SJ, Demanuele C, Debener S, Helps SK, James CJ, Sonuga-Barke EJS. Default-mode brain dysfunction in mental disorders: A systematic review. *Neuroscience & Biobehavioral Reviews*. 2009;33(3):279-296. doi:10.1016/j.neubiorev.2008.09.002

19. Buckner RL, Andrews-Hanna JR, Schacter DL. *The Brain's Default Network*: *Anatomy, Function, and Relevance to Disease*. *Annals of the New York Academy of Sciences*. 2008;1124(1):1-38. doi:10.1196/annals.1440.011

20. Raichle ME, MacLeod AM, Snyder AZ, Powers WJ, Gusnard DA, Shulman GL. A default mode of brain function. *Proceedings of the National Academy of Sciences*. 2001;98(2):676-682. doi:10.1073/pnas.98.2.676

21. Shulman GL, Fiez JA, Corbetta M, et al. Common Blood Flow Changes across Visual Tasks: 11. Decreases in Cerebral Cortex. 1997;9(5):16.

22. Anticevic A, Gancsos M, Murray JD, et al. NMDA receptor function in large-scale anticorrelated neural systems with implications for cognition and schizophrenia. *Proceedings of the National Academy of Sciences*. 2012;109(41):16720-16725. doi:10.1073/pnas.1208494109

23. Hsiao F-J, Wang Y-J, Yan S-H, Chen W-T, Lin Y-Y. Altered Oscillation and Synchronization of Default-Mode Network Activity in Mild Alzheimer's Disease Compared to Mild Cognitive Impairment: An Electrophysiological Study. Lin C-P, ed. *PLoS ONE*. 2013;8(7):e68792. doi:10.1371/journal.pone.0068792

24. Sripada C, Kessler D, Fang Y, Welsh RC, Prem Kumar K, Angstadt M. Disrupted network architecture of the resting brain in attention-deficit/hyperactivity disorder: Disrupted Network Architecture in ADHD. *Human Brain Mapping*. 2014;35(9):4693-4705. doi:10.1002/hbm.22504

25. Tang Y, Xia W, Yu X, et al. Altered cerebral activity associated with topiramate and its withdrawal in patients with epilepsy with language impairment: An fMRI study using the verb generation task. *Epilepsy & Behavior*. 2016;59:98-104. doi:10.1016/j.yebeh.2016.03.013

26. Wandschneider B, Burdett J, Townsend L, et al. Effect of topiramate and zonisamide on fMRI cognitive networks. *Neurology*. 2017;88(12):1165-1171. doi:10.1212/WNL.0000000000003736

27. Yasuda CL, Centeno M, Vollmar C, et al. The effect of topiramate on cognitive fMRI. *Epilepsy Research*. 2013;105(1-2):250-255. doi:10.1016/j.eplepsyres.2012.12.007

28. Laufs H, Krakow K, Sterzer P, et al. Electroencephalographic signatures of attentional and cognitive default modes in spontaneous brain activity fluctuations at rest. *Proceedings of the National Academy of Sciences*. 2003;100(19):11053-11058. doi:10.1073/pnas.1831638100

29. Mantini D, Perrucci MG, Del Gratta C, Romani GL, Corbetta M. Electrophysiological signatures of resting state networks in the human brain. *Proceedings of the National Academy of Sciences*. 2007;104(32):13170-13175. doi:10.1073/pnas.0700668104

30. Neuner I, Arrubla J, Werner CJ, et al. The Default Mode Network and EEG Regional Spectral Power: A Simultaneous fMRI-EEG Study. Chialvo DR, ed. *PLoS ONE*. 2014;9(2):e88214. doi:10.1371/journal.pone.0088214

31. Scheeringa R, Bastiaansen MCM, Petersson KM, Oostenveld R, Norris DG, Hagoort P. Frontal theta EEG activity correlates negatively with the default mode network in resting state. *International Journal of Psychophysiology*. 2008;67(3):242-251. doi:10.1016/j.ijpsycho.2007.05.017

32. Scheeringa R, Petersson KM, Oostenveld R, Norris DG, Hagoort P, Bastiaansen MCM. Trial-by-trial coupling between EEG and BOLD identifies networks related to alpha and theta EEG power increases during working memory maintenance. *NeuroImage*. 2009;44(3):1224-1238. doi:10.1016/j.neuroimage.2008.08.041

33. Das A, de los Angeles C, Menon V. *Electrophysiological Foundations of the Human Default-Mode Network Revealed by Brain-Wide Intracranial-EEG Recordings during Resting-State and Cognition*. Neuroscience; 2020. doi:10.1101/2020.07.24.220566

34. Fox KCR, Foster BL, Kucyi A, Daitch AL, Parvizi J. Intracranial Electrophysiology of the Human Default Network. *Trends in Cognitive Sciences*. 2018;22(4):307-324. doi:10.1016/j.tics.2018.02.002

35. Grech R, Cassar T, Muscat J, et al. Review on solving the inverse problem in EEG source analysis. *Journal of NeuroEngineering and Rehabilitation*. 2008;5(1):25. doi:10.1186/1743-0003-5-25

36. Pascual-Marqui RD, Lehmann D, Koukkou M, et al. Assessing interactions in the brain with exact low-resolution electromagnetic tomography. *Philosophical Transactions of the Royal Society A: Mathematical, Physical and Engineering Sciences*. 2011;369(1952):3768-3784. doi:10.1098/rsta.2011.0081

37. Calhoun VD, Adali T. Multisubject Independent Component Analysis of fMRI: A Decade of Intrinsic Networks, Default Mode, and Neurodiagnostic Discovery. *IEEE Reviews in Biomedical Engineering*. 2012;5:60-73. doi:10.1109/RBME.2012.2211076

38. Hyvärinen A, Oja E. Independent ComponentAnalysis Algorithms and Applications. *Neural Networks*. Published online April 1999.

39. Calhoun VD, Liu J, Adalı T. A review of group ICA for fMRI data and ICA for joint inference of imaging, genetic, and ERP data. *NeuroImage*. 2009;45(1):S163-S172. doi:10.1016/j.neuroimage.2008.10.057

40. Huster RJ, Plis SM, Calhoun VD. Group-level component analyses of EEG: validation and evaluation. *Frontiers in Neuroscience*. 2015;9. doi:10.3389/fnins.2015.00254

41. Pascual-Marqui RD, Kochi K, Lehmann D, Koukkou M, Kinoshita T. Functional independent components: revealing cortico-cortical, cross-frequency interactions. *Japanese Journal of Pharmaco-EEG*. 2011;(12):53-58.

42. Aoki Y, Ishii R, Pascual-Marqui RD, et al. Detection of EEG-resting state independent networks by eLORETA-ICA method. *Frontiers in Human Neuroscience*. 2015;9. doi:10.3389/fnhum.2015.00031

43. Gerrits B, Vollebregt MA, Olbrich S, et al. Probing the "Default Network Interference Hypothesis" With EEG: An RDoC Approach Focused on Attention. *Clinical EEG and Neuroscience*. 2019;50(6):404-412. doi:10.1177/1550059419864461

44. Milz P, Faber PL, Lehmann D, Koenig T, Kochi K, Pascual-Marqui RD. The functional significance of EEG microstates—Associations with modalities of thinking. *NeuroImage*. 2016;125:643-656. doi:10.1016/j.neuroimage.2015.08.023

45. Wang X-J. Neurophysiological and Computational Principles of Cortical Rhythms in Cognition. *Physiological Reviews*. 2010;90(3):1195-1268. doi:10.1152/physrev.00035.2008

46. Jensen O, Kaiser J, Lachaux J-P. Human gamma-frequency oscillations associated with attention and memory. *Trends in Neurosciences*. 2007;30(7):317-324. doi:10.1016/j.tins.2007.05.001

47. Groppe DM, Bickel S, Keller CJ, et al. Dominant frequencies of resting human brain activity as measured by the electrocorticogram. *NeuroImage*. 2013;79:223-233. doi:10.1016/j.neuroimage.2013.04.044

48. Sternberg S. High-Speed Scanning in Human Memory. *Science*. 1966;153(3736):652-654. doi:10.1126/science.153.3736.652

49. Subramanian M, Birnbaum AK, Remmel RP. High-Speed Simultaneous Determination of Nine Antiepileptic Drugs Using Liquid Chromatography-Mass Spectrometry: *Therapeutic Drug Monitoring*. 2008;30(3):347-356. doi:10.1097/FTD.0b013e3181678ecb

50. Benton A. *BASIC APPROACHES TO NEUROPSYCHOLOGICAL ASSESSMENT*.; 1991:505-523.

51. Lezak MD, Howieson DB. *Neuropsychological Assessment*. 4th ed.. Oxford University Press; 2004.

52. Wechsler D. *Wechsler Adult Intelligence Scale–Fourth Edition (WAIS–IV)*. Psychological Corporation; 2014.

53. Mullen T. *CleanLine EEGLAB Plugin*.; 2012.

54. Mazziotta J, Toga A, Evans A, et al. A probabilistic atlas and reference system for the human brain: International Consortium for Brain Mapping (ICBM). Kötter R, ed. *Philosophical Transactions of the Royal Society of London Series B: Biological Sciences*. 2001;356(1412):1293-1322. doi:10.1098/rstb.2001.0915

55. Pascual-Marqui RD. Discrete, 3D distributed, linear imaging methods of electric neuronal activity. Part 1: exact, zero error localization. *arXiv:07103341 [math-ph, physics:physics, q-bio]*. Published online October 18, 2007. Accessed October 4, 2020. http://arxiv.org/abs/0710.3341

56. Jatoi MA, Kamel N, Malik AS, Faye I. EEG based brain source localization comparison of sLORETA and eLORETA. *Australasian Physical & Engineering Sciences in Medicine*. 2014;37(4):713-721. doi:10.1007/s13246-014-0308-3

57. Mauchly JW. Significance Test for Sphericity of a Normal n-Variate Distribution. *The Annals of Mathematical Statistics*. 1940;11(2):204-209. doi:10.1214/aoms/1177731915

58. Helwig NE. *Nonparametric Tests*.; 2019.

59. Helwig NE. Statistical nonparametric mapping: Multivariate permutation tests for location, correlation, and regression problems in neuroimaging. *Wiley Interdisciplinary Reviews: Computational Statistics*. 2019;11(2):e1457. doi:10.1002/wics.1457

60. Winkler AM, Ridgway GR, Webster MA, Smith SM, Nichols TE. Permutation inference for the general linear model. *NeuroImage*. 2014;92:381-397. doi:10.1016/j.neuroimage.2014.01.060

61. Winkler AM, Webster MA, Vidaurre D, Nichols TE, Smith SM. Multi-level block permutation. *NeuroImage*. 2015;123:253-268. doi:10.1016/j.neuroimage.2015.05.092

62. Milz P, Pascual-Marqui RD, Lehmann D, Faber PL. Modalities of Thinking: State and Trait Effects on Cross-Frequency Functional Independent Brain Networks. *Brain Topography*. 2016;29(3):477-490. doi:10.1007/s10548-016-0469-3

63. Smith SM, Fox PT, Miller KL, et al. Correspondence of the brain's functional architecture during activation and rest. *Proceedings of the National Academy of Sciences*. 2009;106(31):13040-13045. doi:10.1073/pnas.0905267106

64. Job A, Paucod J-C, O'Beirne GA, Delon-Martin C. Cortical representation of tympanic membrane movements due to pressure variation: An fMRI study. *Human Brain Mapping*. 2011;32(5):744-749. doi:10.1002/hbm.21063

65. Saur D, Kreher BW, Schnell S, et al. Ventral and dorsal pathways for language. *Proceedings of the National Academy of Sciences*. 2008;105(46):18035-18040. doi:10.1073/pnas.0805234105

66. Narayanan NS, Laubach M. Top-Down Control of Motor Cortex Ensembles by Dorsomedial Prefrontal Cortex. *Neuron*. 2006;52(5):921-931. doi:10.1016/j.neuron.2006.10.021

67. Du J, Rolls ET, Cheng W, et al. Functional connectivity of the orbitofrontal cortex, anterior cingulate cortex, and inferior frontal gyrus in humans. *Cortex*. 2020;123:185-199. doi:10.1016/j.cortex.2019.10.012

68. Rolls ET. The cingulate cortex and limbic systems for emotion, action, and memory. *Brain Structure and Function*. 2019;224(9):3001-3018. doi:10.1007/s00429-019-01945-2

69. Olbrich S, van Dinteren R, Arns M. Personalized Medicine: Review and Perspectives of Promising Baseline EEG Biomarkers in Major Depressive Disorder and Attention Deficit Hyperactivity Disorder. *Neuropsychobiology*. 2015;72(3-4):229-240. doi:10.1159/000437435

70. Yahata N, Kasai K, Kawato M. Computational neuroscience approach to biomarkers and treatments for mental disorders: Computational psychiatry. *Psychiatry and Clinical Neurosciences*. 2017;71(4):215-237. doi:10.1111/pcn.12502

71. Mecarelli O. *Clinical Electroencephalography*. Springer; 2019.